A Plasmonic 2×1 Multiplexerusing an Optical Adder Integrated with a MEMS Micro-Switch

Razieh SoltaniSarvestani[1], Rahim Ghayour*[2], Maryam Mohitpour[3]

Abstract– A2×1Micro-Opto-Electro-Mechanical-Systems (MOEMS)multiplexer consisting of Metal-Insulator-Metal (MIM) waveguides and micro resonators is designed and numerically investigated. The proposed device provides advantages of the Surface Plasmon Polaritons (SPPs) propagation in the MIM structure and a mechanically tunable optical switch to realize the multiplexing function. According to the simulation results, the transmittances of the output channels of the device reach up to72% at the desired wavelengths. Thereafter, the geometry of the proposed structure has been optimized to improve its functional characteristics. An extinction ration around 25.6 dBis obtained for the optimized two-channel structure in the operating wavelength range. Simple fabrication processes, high efficiency, and low-cost manufacturing process make the proposed micro device a suitable choice for several applications in optical telecommunications, especially wavelength division multiplexing.

1. Introduction

In recent years, Surface Plasmon Polaritons (SPPs)-based Metal–Insulator–Metal (MIM) waveguides have offered significant interest due to their unique properties. One property of SPPs is their ability to guide optical signals along metal–dielectric interfaces, while confining and controlling the propagating field within nano scale dimensions. In fact, application of such an approach can overcome the traditional diffraction limit of their dielectric counterparts. An MIM structure offers other advantages including deep sub-wavelength confinement of light, creation of good balance between propagation length and loss, as well as ease of integration on a microchip[1-3].Therefore, SPPs-based MIM waveguides are promising platforms for high speed and ultra-compact optical telecommunication circuits and systems. Today, a plenty of plasmonic structures have been proposed for a wide range of applications, including filters[4], sensors[5], demultiplexers[6],switches[7], logicgates[8],etc. Although

1,3 Department of Electrical Engineering, Shiraz Branch, Islamic Azad University, Shiraz, Iran.

2* Corresponding Author : Department of Electrical Engineering, Shiraz Branch, Islamic Azad University, Shiraz, Iran Email: rghayour@shirazu.ac.ir

these structures can be realized using other techniques such as silicon photonic technology or photonic crystals, the plasmonic structures occupy a much smaller area comparing to the mentioned platforms[9, 10].

Among the above-mentioned structures, multiplexers play a vital role in Wavelength-Division-Multiplexing (WDM) systems as they can enable efficient and cost-effective transmission of multiple signals over a single communication channel as the main part of optical telecommunication systems[6].WDM is a useful technique that can transmit different wavelengths in both directions over a single channel (e.g., optical fiber) and multiplexes them accordingly. Finally, the multiplexed signal is demultiplexed on the end side of transmission using a demultiplexer to separate them as individual signals including unique massages. Many studies have so far been performed on the design of plasmonic demultiplexers. Yaw-Dong Wu et al. proposed a wavelength demultiplexing structure based on an array of MIM plasmonic ring resonators[11]. In a similar study, Huang et al. have suggested a wavelength demultiplexing structure based on plasmonic MIM side-coupled cavities [12]. Another contribution presents a four-channel plasmonic demultiplexer based on add-drop filters consisting of H-shaped resonant cavities on a gold–air–gold structure[13]. Two other designs of tunable plasmonic multi-channel

demultiplexers based on graphene sheets and ring resonators are proposed and numerically investigated[14, 15]. These structures suffer from the low optical transmission efficiency and the difficulty of the fabrication process. Alternatively, there are other types of nano-cavity-based demultiplexers that use graphene nano-ribbons to realize tunable waveguides and optical nano-cavities [16, 17]. The main advantage of these demultiplexers lies in their tunability via external signal.

Although there are a lot of MIM structures proposed for demultiplexing function, there are not so many research studies on the design of plasmonic multiplexers as they need an external controlling signal to choose one of the input signals to be guided through the bus waveguide. The controlling section which usually contains a non-linear optical material called the switch section. So far, several structures containing nonlinear optical materials have been suggested for all-optical nano-plasmonic switches. Emami et.al. proposed an optical switch based on a split square ring resonator and straight waveguides[18]. Furthermore, ahybrid all-optical infrared MIM switch incorporating photonic crystal bandgap structures is proposed byKhani et.al.[19]. Bana et.al and Nurmohammadi et.al. took the advantage of ring resonators coupled to straight waveguides to develop a nano-plasmonic switch[20, 21]. Khani et.al. presented an all optical switch based on asymmetric directional couplers filled with Kerr nonlinear material incorporating Bragg gratings[22]. An all-optical plasmonic switch based on Fano resonance in an X-shaped resonator coupled to parallel stubs proposed byKarimi et.al.[23]. Most of the above-mentioned devices are composed of side-coupled resonators filled with a Kerr nonlinear material and a pump light source to perform the switching function.

All-optical switching schemes that are based onside-couplednano-plasmonic resonators have compact dimensions and due to their relatively low-level of pumping powers requirement, are one of the best choices for designing all-optical multiplexers. For instance, Fasihi et.al. proposed a novel MIM-based 2×1 multiplexer, including an adder module and an all-optical controllable nano-plasmonic switch using a Kerr non-linear material. In their study they have shown that by applying a pump light, the transmissions of the input signals into the output waveguide can be efficiently controlled due to application of the nonlinear nature of Kerr material inside the plasmonic resonator[24].There is also another type of plasmonic optical multiplexer called mode multiplexer which provides mode conversion and multiplexing[25],which is beyond the discussion of this paper.

The main disadvantage of the above-mentioned all

optical switches and multiplexers is to have an external pump signal in the switching part which makes the device more sophisticated and expensive. Besides, there are other disadvantages including the dependence of response upon the wavelength of pump light, including a waveguide line to guide the pump to the Kerr filled resonator, the need to filter the pump signal from the output using optical resonators, and relatively high power consumption[22, 24]. To overcome these issues, one can suggest Micro-Electro-Mechanical-Systems (MEMS) to realize the switch part of the multiplexer. By such an approach, the overall cost and the complexity of the device can be reduced and the power consumption decreases significantly.

In this paper, a novel topology is proposed to realize an optical MIM multiplexer which uses a micro mechanical structure in combination with MIM waveguides and resonators to realize switching and wavelength selecting features. The proposed device contains a simple structure and small footprint which resulting in a low-cost fabrication process. Additionally, the use of electrostatic force to achieve a mechanically tunable cavity enhances its performance, particularly in terms of power consumption. Moreover, the proposed structure supports relatively narrow-band transmission peaks with low crosstalk which is desirable for optical-communication applications including WDM.

The remaining of this paper is as follows: the second section is dedicated to the introduction of the proposed structure and explanation of its main features. In the third section, the numerical method and materials are discussed. Results obtained from the simulations are presented in the fourth section, and the dependencies of the behavior on all structural parameters are analyzed in detail. Moreover, to investigate the characteristics of the plasmonic MIM part of the device we use a FDTD method and an analytical process is used to design the mechanical part. Finally, the fifth section includes summary and some concluding remarks.

2. **Structure and theory**

The proposed structure is composed of two main parts: a MEMS-based adder and a plasmonic switch. Fig. 1shows a 3D schematic of the proposed micro-device. The adder section consists of two air filled straight waveguides called input channels, and two rectangular resonators. Each channel supports only a single wavelength peak in the target wavelength range which can be customized in compliance with the desired optical communication network requirements. According to the schematic of the standard multiplexer depicted in Fig. 2-a, the air-filled

straight waveguides are the input channels, the right side of the bus waveguide is the output port and the external applied voltage is applied as the control signal, that determines the required channel to be selected and guided through the bus waveguide.
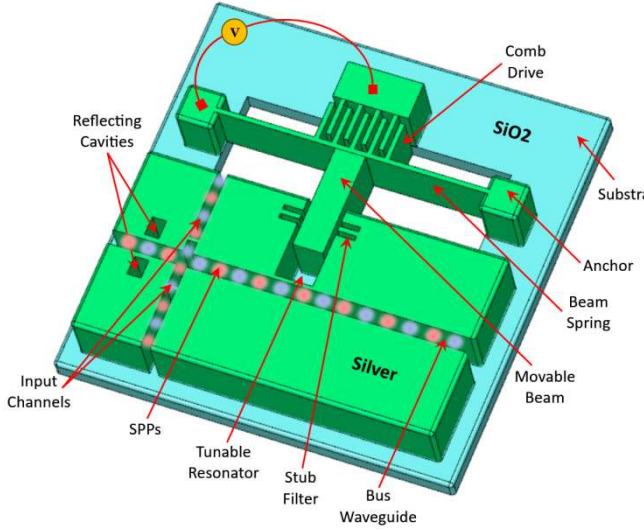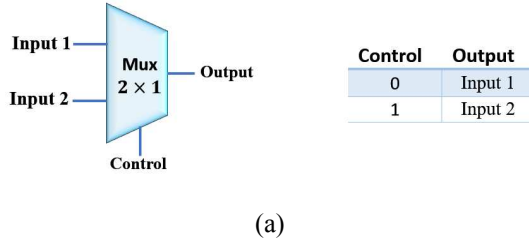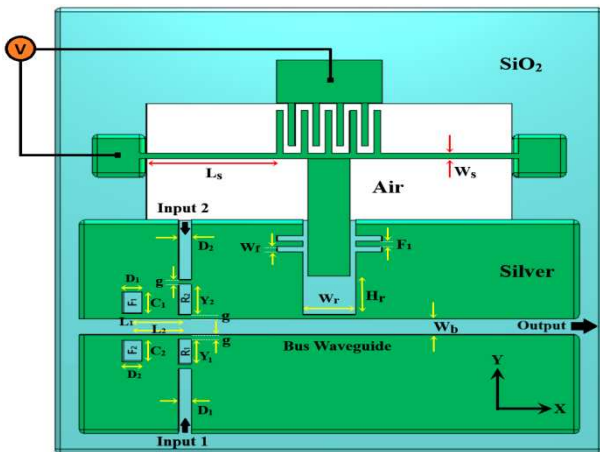

Fig. 1: A 3D schematic of the proposed 2×1 multiplexer including MEMS switch and optical adder.

(a)

(b)

Fig. 2: A 2D schematic of the proposed 2×1 multiplexer. a) schematic of a general multiplexer. b) The upper part is the MEMS-based switch, and the lower part is the optical adder. Here, R_1 and R_2 are channel resonators and F_1 and F_2 are reflecting resonators.

Using this structure, the input optical signals with different wavelength ranges are coupled to the bus waveguide and combined alternatively. To enhance the transmission efficiency of the optical adder, two rectangular reflecting cavities acting as feedback resonators are placed on the left side of the bus waveguide. The transmission wavelength of the channels canbe described using the following formula [12]:

$$\lambda_m = 2\,n_{eff} \frac{L}{m - \frac{\phi_r}{2\pi}} \tag{1}$$

where m corresponds to the order of the optical resonant mode, L is the length of the cavity, n_{eff} is the effective refractive index of the MIM waveguide at the desired wavelength, and ϕ_r is the phase shift of the beam reflected at one end of the resonant cavity.

The switch section consists of an air-filled rectangular resonator coupled to the bus waveguide, which absorbs one of the input modes and allows the other to pass through. As a matter of fact, the excited guided modes at the frequencies near the resonance frequency of this side-coupled rectangular resonator can be coupled into the cavity and then decoupled into the bus waveguide. This action results in transmission dips in the output spectrum of the bus waveguide, due to the destructive interference. Because the central wavelengths of the resonant modes are mainly determined by the size and the effective refractive index of this rectangular resonator, one can realize an optical switch by simply changing its length instead of changing its refractive index using Kerr nonlinear material. The transmission spectrum of the switch part obeys the following equation which is a general formula describing the response of a resonator that is side coupled to a waveguide[24]:

$$
\begin{aligned}
T = |t|^2 &= \frac{p_{out}}{p_{in}} \\
&= \frac{(p_{in} - p_{out} - \delta)^2 + (\tau/\tau^{'})}{(p_{in} - p_{out} - \delta)^2 + 1}
\end{aligned}
\tag{2}
$$

where defining $1/\tau = 1/\tau_0 + 1/\tau_e$ and $1/\tau^{'} = 1/\tau_0 - 1/\tau_e$, $\delta = \tau(\omega_0 - \omega)$, t is the transfer function, $1/\tau_0$ is the intrinsic resonator decay rate, $1/\tau_e$ is the decay rate due to the escaping power, P_{in} is the input power and P_{out} stands for the output power. The principle behind the design of this switch is known as "critical coupling". This occurs at the resonance frequency when $\tau_0 = \tau_e$, while assuming the

transfer function becomes zero.

Moreover, when the resonant wavelength of channel 1 is chosen equal to the resonant wavelength of rectangular resonator, only the mode supported by channel 2 appears on the output side. In contrast, when the size of the rectangular cavity supports the resonance wavelength of channel 2, only channel one's mode can travel through the output port. Therefore, it is adequate to tune the rectangular cavity in terms of size to activate the optical switch alternatively, where the proposed configuration can be realized using a MEMS structure (see Fig. **3**).
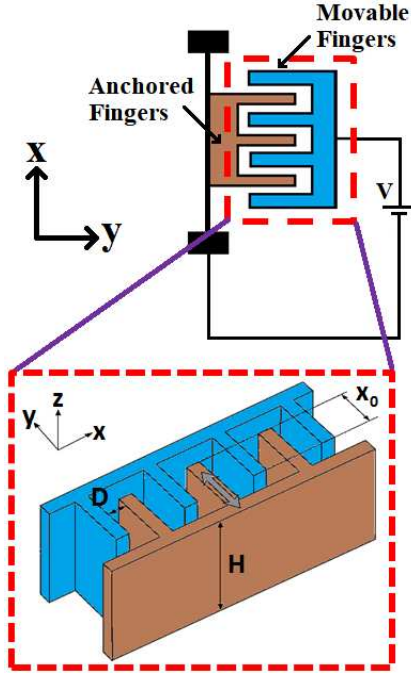
Fig. 3: 2D and 3D schematic of the comb-drive actuator used in the proposed multiplexer. In this design, anchored comb (brown)is fixed in its position while movable comb (blue) displaces along Y axis. D is the distance between adjacent fingers of fixed and moveable combs, H is the height of the structural layer, and X_0 is the initial active length of the adjacent fingers[26].

To realize the switch part, a comb-drive MEMS actuator is used to adjust the length of the side-coupled resonator. Once a positive voltage is applied to the comb-drive actuator, the electro-static force displaces the movable part along Y-axis. Consequently, the length of the rectangular resonator is changed and sets the required central wavelength of the resonant modes. Therefore, by adjusting the external applied voltage, one can select which guided mode to be omitted and which one to be transmitted to the right side of the bus waveguide. In fact, the electromagnetic properties of the structure are strongly affected through mechanical movements of the moveable comb. The mechanical behavior of the movable comb of the actuator that is governing by the electrostatic force is described using the following formulas[26, 27]:

$$\frac{D_y}{} = \frac{N\,H\,\varepsilon\,\varepsilon_0}{k_y\,D}V^2 \tag{3}$$

$$\frac{k_y}{} = \frac{E\,H\,W_s^3}{4\,L_s^3} \tag{4}$$

whereD_y is the displacement of the movable section of the comb-drive actuator,N is the number of active electrodes, D is the lateral distance between adjacent stationary and movable electrodes. Also,ε is the relative permittivity of surrounding medium, ε_0 is the absolute permittivity of vacuum, k_y is the stiffness coefficient of the simple springs along y axis, E is the Young's module of silver, H is the thickness of the structural layer, L_s is the length of the simple beam spring, W_s is the width of the simple beam spring, and V is the applied external voltage.

For the movable part to move easily inside the structure and change the length of the resonators, the presence of an air gap between the movable part and the frame is required. This gap on the other hand leads to the undesired coupling of the optical signal out of the rectangular resonator which may result ina strong drop in the amplitude of the signal transmitted to the output. To prevent this signal loss and enhance the transmission efficiency of the structure, a pair of double stub structures has been located on the right and left sides of the gap between frame and the movable wall of the rectangular resonator. These stubs act like nearly ideal mirrors in the operating range of the micro-device. By using an analytic model based on the scattering matrix theory, the transmission coefficient of the structure can be calculated. Quantitatively, the scattering property of the double stub resonator for the incident SPPs at a frequency of $\omega = c/\lambda$ can be described by the following transfer matrices, where the transmittance of the system is expressed by $|1/T_{total}|^2$[28]:

$$
\begin{aligned}
T_{total} =& \begin{bmatrix} 1 - \dfrac{i\delta}{\omega - \omega_0} & \dfrac{-i\delta}{\omega - \omega_0} \\ \dfrac{i\delta}{\omega - \omega_0} & 1 + \dfrac{i\delta}{\omega - \omega_0} \end{bmatrix} \times \begin{bmatrix} \exp(i\varphi) & 0 \\ 0 & \exp(-i\varphi) \end{bmatrix} \\
&\times \begin{bmatrix} 1 - \dfrac{i\delta}{\omega - \omega_0} & \dfrac{-i\delta}{\omega - \omega_0} \\ \dfrac{i\delta}{\omega - \omega_0} & 1 + \dfrac{i\delta}{\omega - \omega_0} \end{bmatrix}
\end{aligned} \tag{5}
$$

3. Simulations and materials

To investigate the optical response of the proposed

device, the suggested structure has been numerically analyzed using an FDTD solver. The simulation is done in 2-dimensional approach, while the PMC boundary conditions are selected along all axes.

The target wavelength range is spanned from 200 to 1300 nm and the "number of resulting data samples" is chosen to be 2000. A plane wave with an electric component parallel to the Y-axis is radiated perpendicularly onto the input port to excite the fundamental TM mode of the waveguide. The field profile ports are chosen to collect the propagated light-wave through the bus waveguides as well as output channels. The scattering parameters ($S_{11} - S_{22}$), have been used to obtain the reflection and transmission spectra in the desired wavelength range. For the purpose of numerical analysis, the default relative permittivity of air is taken as 1 and the metal used in the devices is silver with a relative permittivity characterized by Drude model, as follows[12]:

$$\varepsilon(\omega) = \varepsilon_\infty - \frac{\omega_p^2}{\omega(\omega + i\gamma_0)} \tag{6}$$

where $\varepsilon_\infty = 3.7$ is the dielectric constant at the infinite frequency,$\gamma_0 = 0.018\ eV$ is theelectron relaxation rate and $\omega_p = 9.1\ eV$ is the bulk plasma frequency.

4. Design and analysis

As mentioned before, the proposed multiplexer consists of an optical adder and a MEMS-based optical switch. The whole device is designed to work in the IR region of the spectrum. The adder module is designed and analyzed using a FDTD method and then optimized to get a maximum transmission efficiency. The widths of the input waveguides and their resonators(W)are set to50 nm. The silver gap between nano-resonators and the channel waveguides, as well as the coupling gap between nano-resonators and the bus waveguide, are chosen to beg = 10nm. These dimension settings are done to achieve maximum coupling efficiency as well as maximum resonant efficiency. Geometrical parameters of the proposed multiplexer are listed in Table 1.

Simulation results show that input channels in combination with their cavities act as band-pass filters with narrow line widths at the IR region of spectrum. The transmission spectra of the signals coupled from channels to the bus waveguide are calculated and shown in Fig. **4**. The central wavelengths of channels 1 and 2 are 785 nm and 892 nm, while they propagate through the device with transmittances of 72% and 69%,respectively. As depicted in this Figure, this high transmission ensures low insertion-

loss and enhanced extinction-ratio[29, 30]. As mentioned previously to improve the transmission efficiencies of the input channels in the optical adder section, we adjust the position of two side-coupled resonators with respect to the nanoribbon resonators. In fact, these resonators act as two different wavelength-selective reflectors which are placed at the distances L_1 and L_2 from the nanoribbon resonators 1 and 2, respectively, (see Figure 2). The sizes of each of the side-coupled reflecting resonators are the same as the sizes of the corresponding channel resonator.

Table 1: Geometrical parameters of the proposed multiplexer shown in Fig. 2

| Parameter	Symbol	Value [nm]
Width of input waveguide of channel 1	D_1	50
Length of input resonator of channel 1	Y_1	240
Width of input waveguide of channel 2	D_2	50
Length of input resonator of channel 2	Y_2	280
Length of reflecting cavity 1	C_1	240
Length of reflecting cavity 2	C_2	280
Gap between input waveguide 1 and resonator 1	g	10
Width of the grooves of the double stub mirror	W_F	50
Gap between grooves of the double stub mirror	F_1	10
Length of tunable rectangular resonator	H_r	574
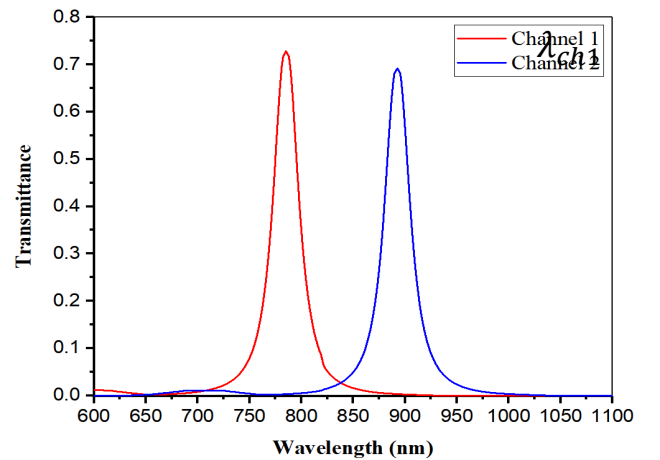
Fig. 4: The transmission spectra of the adder section. The peak wavelengths of channels 1 and 2 are appeared at 785 nm and 892 nm, with transmittances of 72% and 69%, respectively.

As previously discussed, the optical switch section is composed of a bus waveguide side-coupled to a tunable rectangular resonator. Fig. **5** demonstrates the operating principle of this switch based on the dimension of the rectangular resonator. As depicted in this Figure, initially the rectangular resonator supports three perfect resonance peaks in the desired wavelength range at $\lambda_{r1} = 785\ nm$, $\lambda_{r2} = 960\ nm$ and $\lambda_{r3} = 1220\ nm$, with FWHMs around 27 nm, 51 nmand 25 nm.As a matter of fact, the central wavelengths of these resonance peaks are directly related to the dimensions of the rectangular resonator, which can be controlled through the motion of the movable beam along the Y axis. Fig. **5**, also shows the influence of the variations in the width of the rectangular resonator (H_r, shown in Fig. **2**) on the transmission spectrum of the optical switch.
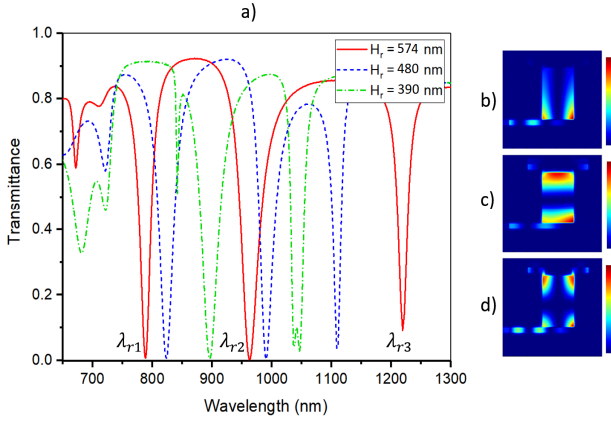
Fig. 5: Spectral behavior and magnetic field profile of the switch section. a) transmission spectra of the switch section for three different values of H_r. Illustration of the Z component of magnetic field profile $|H_z|^2$ of the proposed micro device at wavelengsths of; b) λ_{r1}=785 nm, c) λ_{r2}= 960 nm, d) λ_{r3}= 1220 nm.

In fact, it is useful to analyze the procedure of adjusting the peak and linewidth of each channel. Assume that the dips located at λ_{r1} and λ_{r2} have been selected as the desired dips for switching operation. Now, it is essential to analyze how the size of tunable rectangular resonator affects their central wavelength. As depicted in Fig. **5**-a, by changing the value of H_r, the transmission spectrum of the switch module experiences many changes. For $H_r = 574\ nm$, the central resonance wavelength of tunable resonator λ_{r1} matches that of input channel one (λ_{ch1}=785nm), and for $H_r = 390\ nm$, the central resonance wavelength of tunable resonator λ_{r2} matches that of input channel two ($\lambda_{ch2} = 892$).Hence, a mechanical displacement around $\Delta y = 184\ nm$ should be created by the MEMS actuator to effectively switch the input signals.

Table 2: Geometrical parameters of the MEMS actuator shown in Fig. 3

Parameter	Symbol	Value
Number of Fingers	N	100
Height of the comb-drive actuator	H	200 nm
Distance between adjacent fingers	D	100 nm
Stiffness of the spring along Y axis	k_y	8.59 N/m
Youngs modulus of Silver	E	72.5 GPa
Width of the simple beam spring	W_s	40 nm
Length of the simple beam spring	L_s	300 nm

To realize such a wide range of mechanical tunability, it is important to design the comb-drive actuator in an optimized manner. According to equation 3 and 4, for obtaining $\Delta_y = 184\ nm$, given the structural parameters of the actuator listed in

Table **2**, while the applied voltage should be around $29.9\ V$. Moreover, the actuator is designed such that in its initial state, when there is no displacement due to the application of external voltage, the movable beam is positioned so that the value of H_r is equal to 574 nm which is corresponding to $\Delta_y = 0\ nm$.

To prevent the coupling of the signal from the resonator to the outside, a double stub structure has been added to the side walls of the resonator which act as ideal mirrors in the desired wavelength range (see Fig. **6**). For the geometrical values listed in Table 1, the transmission spectrum of this optical mirror, obtained using FDTD method is demonstrated in Fig. **6**. As shown in this Figure, in the wavelength range of 750 nm to 1300 nm, negligible transmission occurs, meaning that the entire signal reflects upon reaching the double stub mirrors.
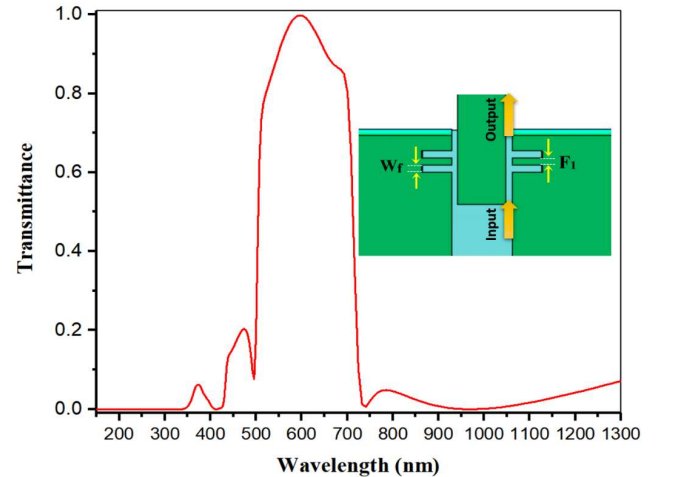
Fig. 6: Transmission spectrum of double stub plasmonic mirrors located on the side walls of the tunable rectangular resonator.

In summary, when a signal with wavelength of $\lambda_{ch1} = 785\ nm$ is applied to channel 1 and a signal with wavelength of $\lambda_{ch2} = 892\ nm$ is applied to channel 2, the SSPs propagate in the channels are then coupled to the bus waveguide. Now, if the external voltage is set to0 volts, the input signal supported by channel 1 is absorbed in the rectangular resonator and only λ_{ch2} appeared in the output port. On the other hand, for V = 29.9 volts, the input signal supported by channel 2 is absorbed in the rectangular resonator and only λ_{ch1} is directly coupled to the output port. The above explained condition is summarized in Table 3.

Table 3: The output signal for different values of external voltage and input signal wavelengths

External Voltage [v]	D_y[nm]	Output
0	0	λ_{ch2}
29.9	184	λ_{ch1}

Another important parameter of any optical multiplexer and switch is Extinction Ratio (ER) which indicates how effectively the device can differentiate between the "on" and "off" states, which is crucial for its performance in optical communication systems. ER is defined by the following formula [29, 30]:

$$ER\ (dB) = 10\ log_{10}\left(\frac{P_{on}}{P_{off}}\right) \tag{7}$$

For our designed structure, ER is calculated to be approximately 21.4 dB for channel one and 25.6 dB for channel two. This indicates that our proposed device performs acceptably when compared to other similar works in this field.

5. Conclusion

To summarize, a2×1 plasmonic multiplexer composed of MIM waveguides and resonators is designed and numerically investigated. Propagation of SPPs in the MIM structure in combination with a mechanically tunable optical switch forms the operation of the proposed device. Simulation results showed that the transmittances of the output peaks are up to 72% and a maximum ERaround25.6 dB are obtained for the optimized structure at the operating wavelength range. The proposed micro device is ideal for various optical telecommunications applications, particularly WDM, due to its simple fabrication process, low production cost, low power consumption and better performance.

References:

[1] B. Beiranvand, A. S. Sobolev, and A. Sheikhaleh, "A proposal for a dual-band tunable plasmonic absorber using concentric-rings resonators and mono-layer graphene," *Optik,* vol. 223, p. 165587, 2020.

[2] M. A. Butt, "Metal-insulator-metal waveguide-based plasmonic sensors: Fantasy or truth—A critical review," *Applied Research,* vol. 2, no. 4, p. e202200099, 2023.

[3] M. A. Butt, N. Kazanskiy, and S. Khonina, "Tapered waveguide mode converters for metal-insulator-metal waveguide plasmonic sensors," *Measurement,* vol. 211, p. 112601, 2023.

[4] N. Korani, A. Abbasi, and M. Danaie, "Band-pass and band-stop plasmonic filters based on Wilkinson power divider structure," *Plasmonics,* vol. 19, no. 2, pp. 733-742, 2024.

[5] M. Danaie, L. Hajshahvaladi, and E. Ghaderpanah, "A single-mode tunable plasmonic sensor based on an 8-shaped resonator for cancer cell detection," *Scientific Reports,* vol. 13, no. 1, p. 13976, 2023.

[6] M. Mohammadi, M. Soroosh, A. Farmani, and S. Ajabi, "High-performance plasmonic graphene-based multiplexer/demultiplexer," *Diamond and Related Materials,* vol. 139, p. 110365, 2023.

[7] S. Pooretemad, M. Pav, Z. Ghattan Kashani, and N. Granpayeh, "Ultra-compact all-optical plasmonic switch for three telecommunication windows using a nonlinear Kerr material and Fano resonance," *Applied Optics,* vol. 62, no. 15, pp. 4123-4133, 2023.

[8] S. H. Abdulwahid, A. G. Wadday, and S. M. Abdulsatar, "Multiple-input hybrid plasmonic OR logic gate with a nanostructure," *Applied Optics,* vol. 62, no. 3, pp. 566-572, 2023.

[9] A. Messner, D. Moor, D. Chelladurai, R. Svoboda, J. Smajic, and J. Leuthold, "Plasmonic, photonic, or hybrid? Reviewing waveguide geometries for electro-optic modulators," *APL Photonics,* vol. 8, no. 10, 2023.

[10] A. Elbanna *et al.*, "2D material infrared photonics and plasmonics," *ACS nano,* vol. 17, no. 5, pp. 4134-4179, 2023.

[11] Y.-D. Wu, "High transmission efficiency wavelength division multiplexer based on metal–insulator–metal plasmonic waveguides," *Journal of Lightwave Technology,* vol. 32, no. 24, pp. 4844-4848, 2014.

[12] X. Mei, X. Huang, J. Tao, J. Zhu, Y. Zhu, and X. Jin, "A wavelength demultiplexing structure based on plasmonic MDM side-coupled cavities," *JOSA B,* vol. 27, no. 12, pp. 2707-2713, 2010.

[13] M. T. H. Azar, M. Zavvari, A. Arashmehr, Y. Zehforoosh, and P. Mohammadi, "Design of a high-performance metal–insulator–metal plasmonic demultiplexer," *Journal of nanophotonics,* vol. 11, no. 2, pp. 026002-026002, 2017.

[14] Q. Deng *et al.*, "Adjustable plasmonic multi-channel demultiplexer with graphene sheets and ring resonators," *Plasmonics,* vol. 14, pp. 993-998, 2019.

[15] S. Asgari and N. Granpayeh, "Tunable plasmonic dual wavelength multi/demultiplexer based on graphene sheets and cylindrical resonator," *Optics Communications,* vol. 393, pp. 5-10, 2017.

[16] H. Zhuang, S. Sheng, F. Kong, K. Li, and Y. Wang, "A wavelength demultiplexing structure based on graphene nanoribbon resonators," *Optics Communications,* vol. 381, pp. 396-402, 2016.

[17] S. Asgari and T. Fabritius, "Tunable mid-infrared graphene plasmonic cross-shaped resonator for demultiplexing application," *Applied Sciences,* vol. 10, no. 3, p. 1193, 2020.

[18] R. Negahdari, E. Rafiee, and F. Emami, "Realization of all-optical plasmonic MIM split square ring resonator switch," *Optical and quantum electronics,* vol. 51, pp. 1-14, 2019.

[19] S. Khani, M. Danaie, and P. Rezaei, "Hybrid all-optical infrared metal-insulator-metal plasmonic switch incorporating photonic crystal bandgap structures," *Photonics and Nanostructures-Fundamentals and Applications,* vol. 40, p. 100802, 2020.

[20] X. Bana, X. Pang, X. Li, B. Hu, Y. Guo, and H. Zheng, "A nonlinear plasmonic waveguide based all-optical bidirectional switching," *Optics Communications,* vol. 406, pp. 124-127, 2018.

[21] T. Nurmohammadi, K. Abbasian, and R. Yadipour, "Ultra-fast all-optical plasmonic switching in near infra-red spectrum using a Kerr nonlinear ring resonator," *Optics Communications,* vol. 410, pp. 142-147, 2018.

[22] S. Khani, M. Danaie, and P. Rezaei, "All-optical plasmonic switches based on asymmetric directional couplers incorporating Bragg gratings," *Plasmonics,* vol. 15, pp. 869-879, 2020.

[23] Y. Karimi, H. Kaatuzian, A. Tooghi, and M. Danaie, "All-optical plasmonic switches based on Fano resonance in an X-shaped resonator coupled to parallel stubs for telecommunication applications," *Optik,* vol. 243, p. 167424, 2021.

[24] S. Bashiri and K. Fasihi, "A 2× 1 all-optical multiplexer using Kerr nonlinear nano-plasmonic switch," *Optical and Quantum Electronics,* vol. 51, no. 11, p. 374, 2019.

[25] M. Yin, Q. Deng, Y. Li, X. Wang, and H. Li, "Compact and broadband mode multiplexer and demultiplexer based on asymmetric plasmonic–

dielectric coupling," *Applied optics,* vol. 53, no. 27, pp. 6175-6180, 2014.

[26] A. Sheikhaleh, K. Jafari, and K. Abedi, "Design and analysis of a novel MOEMS gyroscope using an electrostatic comb-drive actuator and an optical sensing system," *IEEE Sensors Journal,* vol. 19, no. 1, pp. 144-150, 2018.

[27] G. K. Fedder, *Simulation of microelectromechanical systems*. University of California, Berkeley, 1994.

[28] S. Yu, T. Zhao, J. Yu, and D. Pan, "Tuning multiple Fano resonances for on-chip sensors in a plasmonic system," *Sensors,* vol. 19, no. 7, p. 1559, 2019.

[29] F. Moradiani, M. Seifouri, K. Abedi, and F. G. Gharakhili, "High extinction ratio all-optical modulator using a vanadium-dioxide integrated hybrid plasmonic waveguide," *Plasmonics,* vol. 16, no. 1, pp. 189-198, 2021.

[30] A. Udupi and S. K. Madhava, "Plasmonic coupler and multiplexer/demultiplexer based on nano-groove-arrays," *Plasmonics,* vol. 16, no. 5, pp. 1685-1692, 2021.